Figure S1, related to Figure 1.

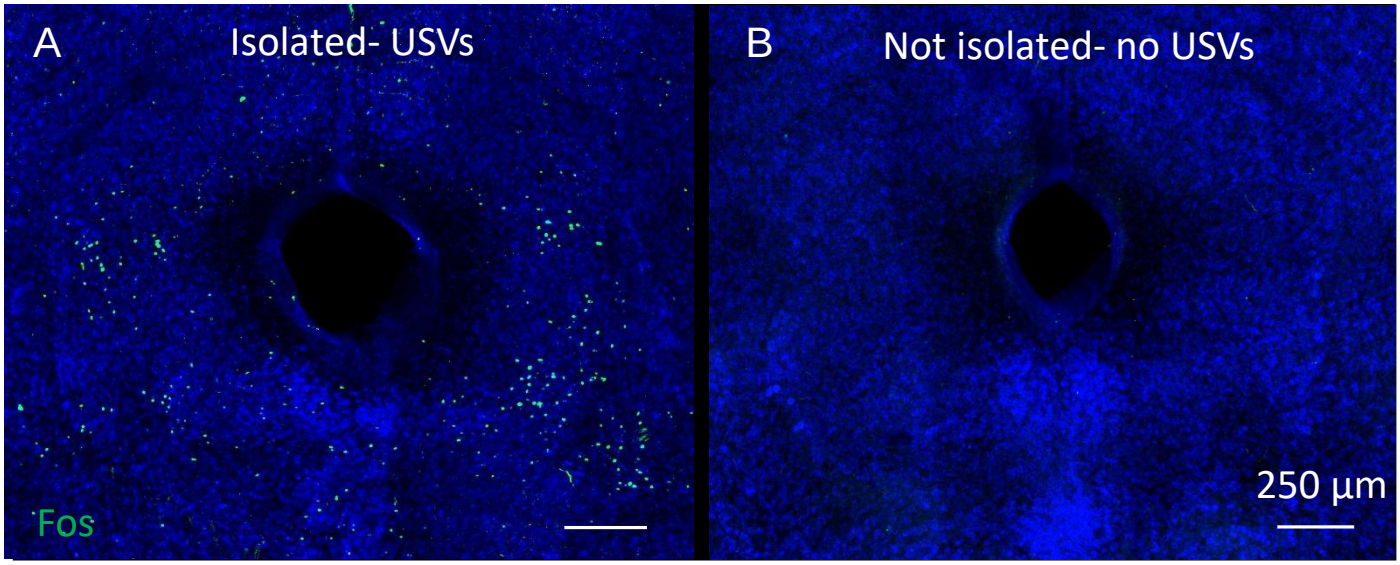

Figure S1, related to Figure 1. The caudolateral PAG contains neurons that upregulate Fos in mouse pups that are isolated from the nest and produce USVs. (A) Representative Fos staining in the caudolateral PAG of a mouse pup that was isolated from the nest and produced USVs (see Methods). (B) Elevated Fos expression was not observed in the caudolateral PAG of pups that were not removed from the nest and did not produce USVs (green, Fos; blue, neuroTrace).

Figure S2, related to Figures 2 and 6.

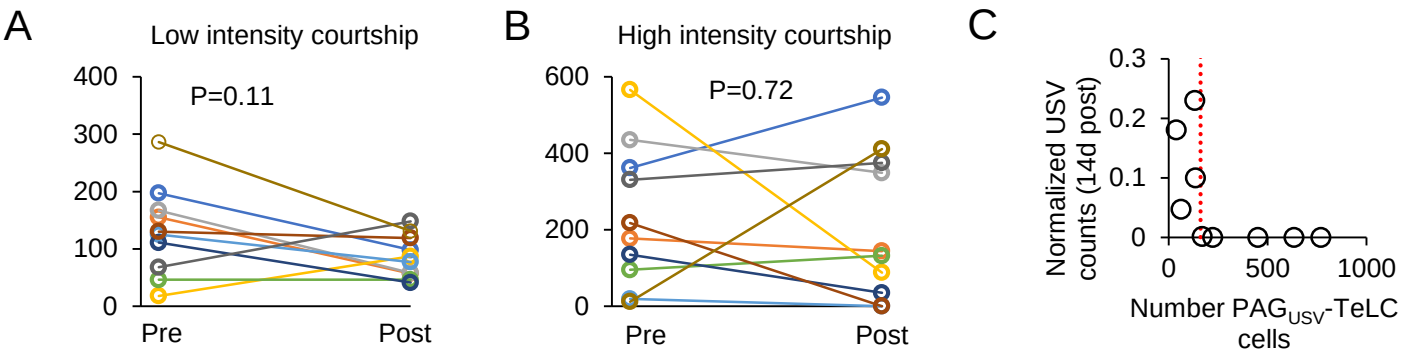

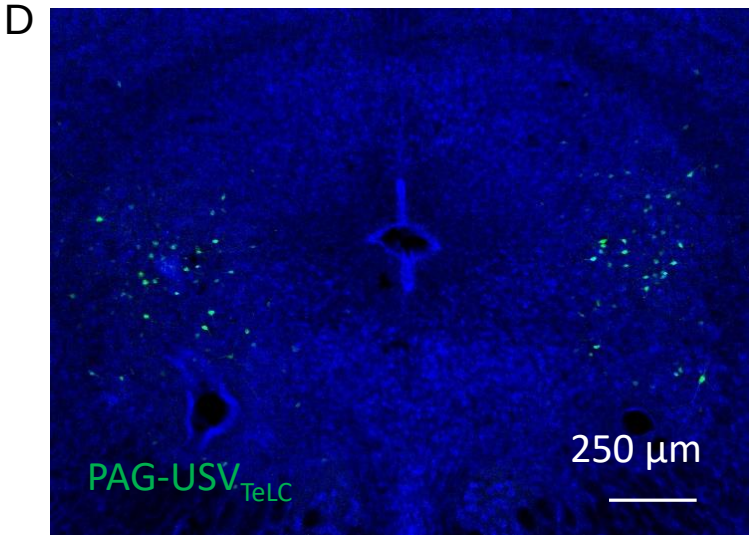

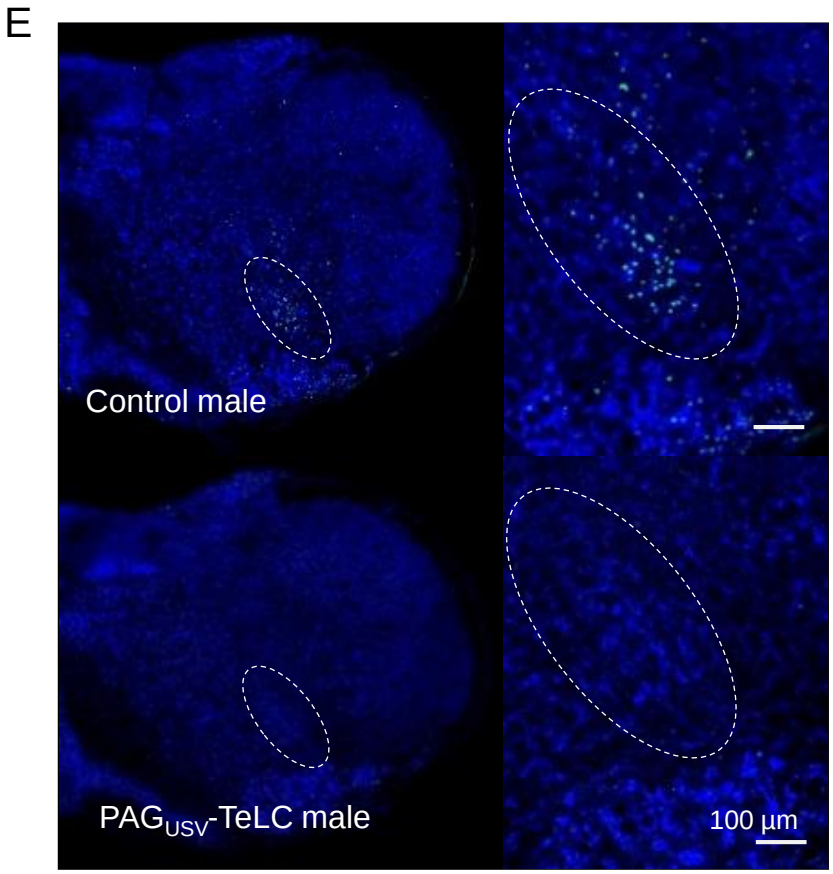

Figure S2, related to Figures 2 and 6. Additional information related to CANE-based silencing of PAG-USV neurons. (A) The amount of time males spend in low intensity courtship (anogenital sniffing and following) is not changed following silencing of PAG-USV neurons (N = 10 males, p = 0.11, Wilcoxon ranked-sign test). (B) Same, for high intensity courtship (i.e., mounting) (p = 0.72). (C) The number of TeLC-expressing PAG-USV neurons is plotted against the normalized USV count for each PAG_{USV}-TeLC male (total day 14 USVs/total day 1 USVs; post-hoc histology quantified for N=9 mice, mean number of infected cells was 289 +/- 88 neurons). (D) Confocal image showing a representative injection of CANE-LV-Cre and AAV-FLEX-TeLC-GFP viruses into the caudolateral PAG. (E) (Top rows) USV-induced Fos expression (green) in RAm is shown for a control male (inset shows magnified view; blue, NeuroTrace). USV-induced Fos in RAm was observed in 10/11 control males. (Bottom rows) USV-induced Fos expression is absent in a male expressing TeLC in PAG-USV neurons. Fos in RAm was observed in 0/5 PAG_{USV}-TeLC males after a 30 minute session with a female.

Figure S3, related to Figure 3.

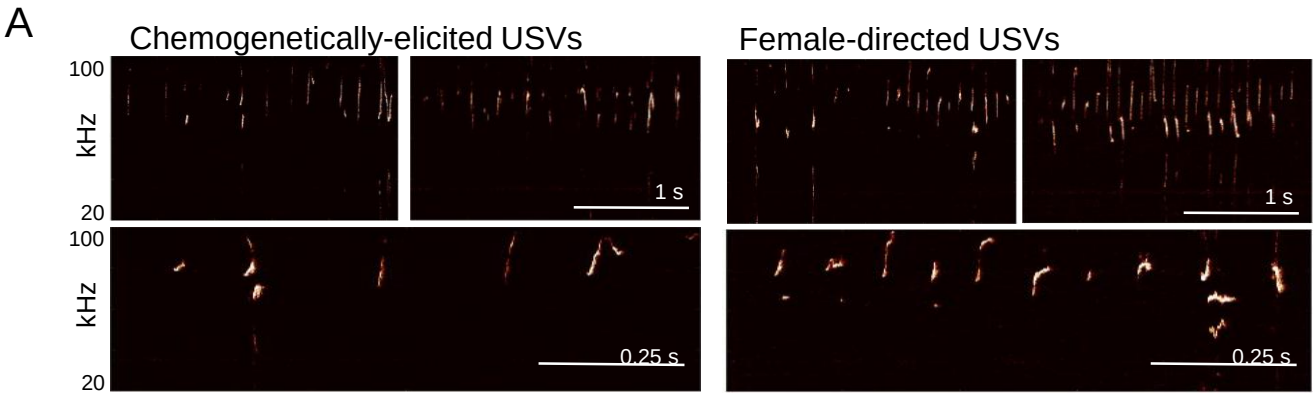

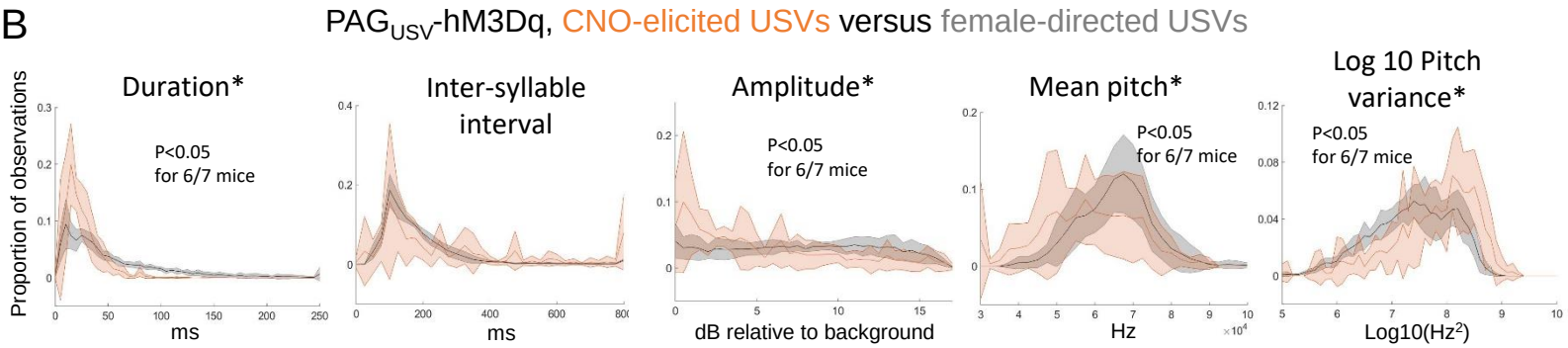

* At least 6 of 7 mice changed median value in same direction

n=17213 female-directed USVs
n=2220 CNO-elicited USVs

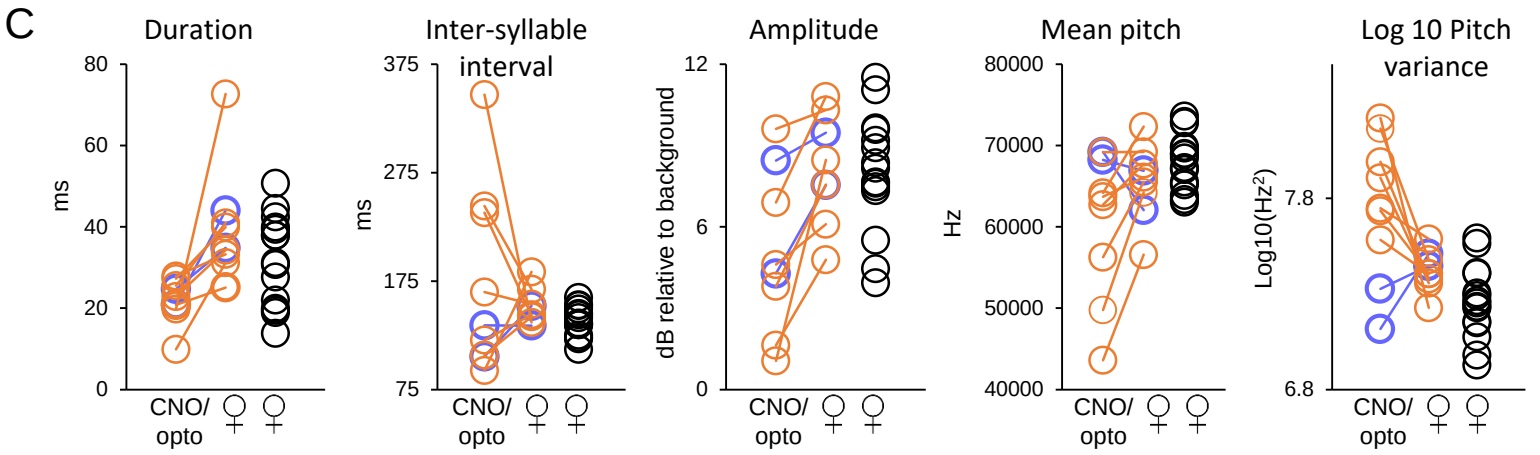

N=7 PAG$_{USV}$-hM3Dq males N=2 PAG$_{USV}$-ChR2 males N=15 control Fos^{TVA} males (n=25338 female-directed USVs)

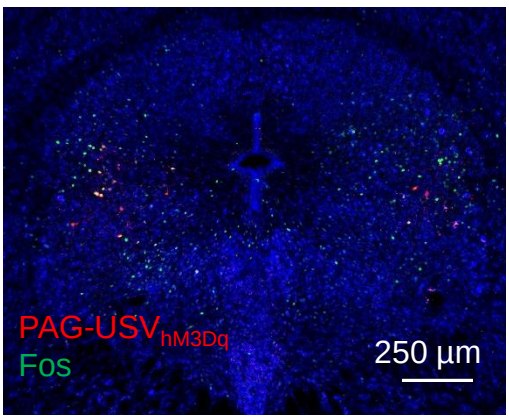

Figure S3, related to Figure 3. Comparison of acoustic features of chemogenetically- and optogenetically-elicited USVs versus courtship USVs. (A) Spectrograms show CNO-USVs (left) and female-directed USVs (right) from the same PAG_{USV}-hM3Dq male. Bottom panels show expanded view from top panels. (B) Distributions of 5 acoustic parameters are shown for CNO-USVs (orange) and female-directed USVs (gray) for 7 PAG_{USV}-hM3Dq mice (lines show mean values, shading represents standard deviation). Asterisks indicate acoustic parameters whose median value changed significantly in the same direction for at least 6 of 7 mice (defined as $p<0.05$ for Mann Whitney U tests performed for a given mouse and acoustic parameter). (C) Distributions of 5 acoustic parameters are shown for optogenetically-elicited USVs (blue) and courtship USVs (gray) for 2 PAG_{USV}-ChR2 mice. Asterisks indicate acoustic parameters whose median value changed significantly in the same direction for both mice ($p<0.05$, Mann Whitney U tests.) (D) Median values of 5 acoustic parameters for CNO-elicited/optogenetically-elicited USVs and courtship USVs from PAG_{USV}-hM3Dq mice (orange connected points) and PAG_{USV}-ChR2 mice (blue connected points) are compared to median values measured from 15 control Fos^{TVA} males producing courtship USVs (black). (D) Confocal image showing a representative injection of CANE-LV-Cre and AAV-hM3Dq-mCherry viruses (mean number of infected neurons was 218 +/- 41).

Figure S4, related to Figure 3.

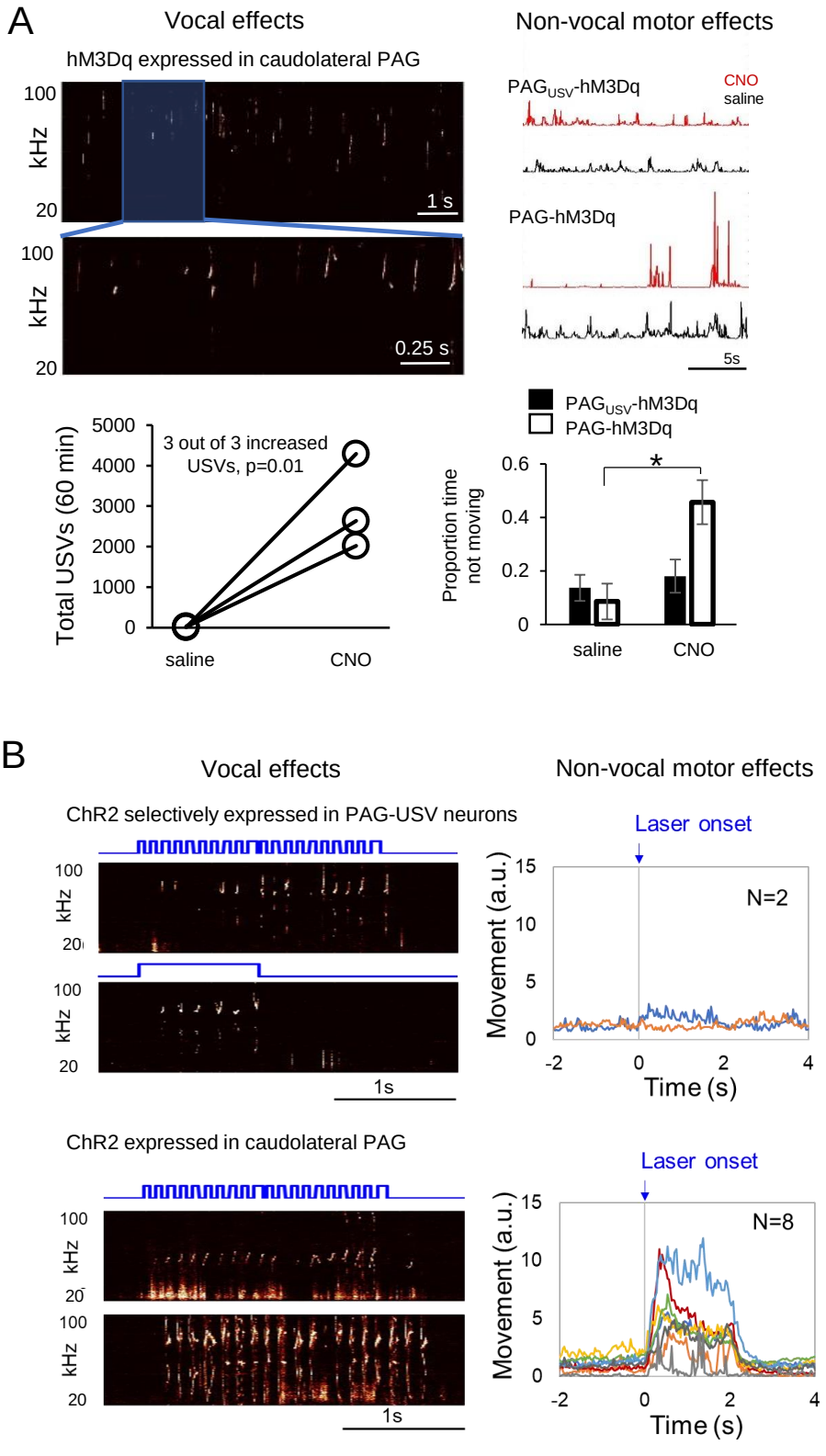

Figure S4, related to Figure 3. Non-selective chemogenetic and optogenetic activation of caudolateral PAG neurons drives USV production as well as non-vocal movements. (A) (Top, left) Spectrograms show USVs produced by a VGlut-Cre male after injection of AAV-FLEX-hM3Dq bilaterally into the caudolateral PAG and treatment with CNO. (Bottom, left) All 3 VGlut-Cre males with hM3Dq expression in the caudolateral PAG dramatically increased USV production following treatment with CNO as compared to saline. (Top, right) Representative movement traces from a PAG_{USV}-hM3Dq male and a PAG-hM3Dq male, after treatment with either CNO (red traces) or saline (black traces). Note that the movement of the PAG-hM3Dq male after CNO treatment consists of periods of immobility punctuated by periods of high speed movement. (Bottom, right) Quantification of proportion of time spent immobile (>1s periods) for PAG_{USV}-hM3Dq (N = 8, black bars) and PAG-hM3Dq males (N = 3, white bars) after treatment with either saline or CNO (two-way repeated measures ANOVA revealed significant interaction between group and treatment, $p = 0.01$ for PAG-hM3Dq CNO versus saline, $p = 0.28$ for PAG_{USV}-hM3Dq CNO versus saline, paired t-tests, mean ± SE are shown). (B) (Top, left) Selective expression of ChR2 in PAG-USV neurons drives USV production during laser stimulation (top, left) but not non-vocal movements (top, right). In contrast, non-selective ChR2 expression of ChR2 in caudolateral PAG neurons drives both USV production (bottom, left) and high speed movements (bottom, right) during laser stimulation (N = 8 mice). Please note that second spectrogram from the example PAG_{USV}-ChR2 mouse is also included in Fig. 3B.

Figure S5, related to Figure 3.

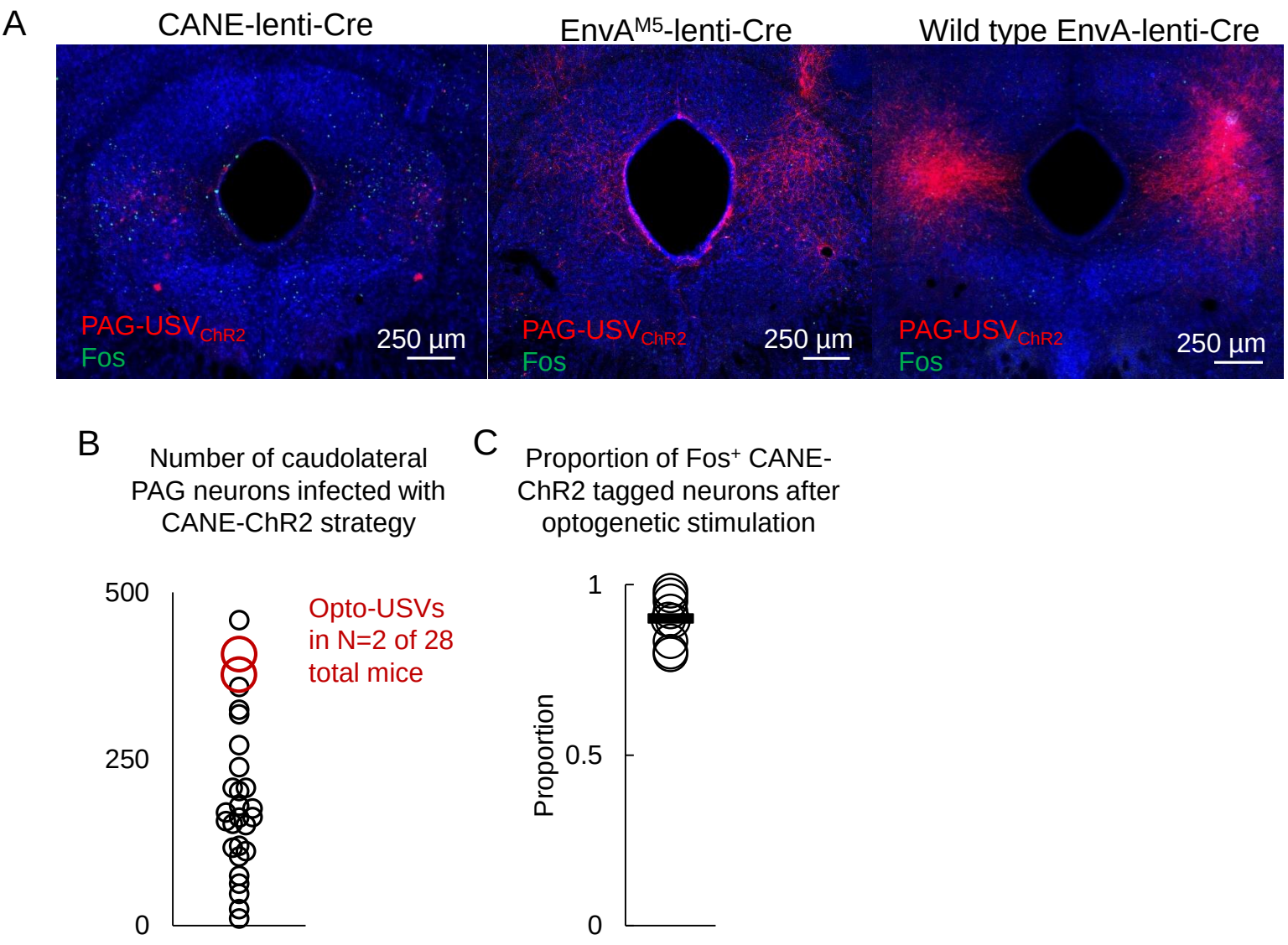

Figure S5, related to Figure 3. Additional information related to optogenetic activation of PAG-USV neurons. (A) Representative confocal images showing viral labeling observed after infection of PAG-USV neurons with AAV-FLEX-ChR2 co-injected with CANE-LV-Cre (left), EnvA^{M5}-LV-Cre (middle), and wild-type EnvA-LV-Cre (right). (B) Quantification of the number of PAG neurons infected after co-injection of AAV-FLEX-ChR2 and CANE-LV-Cre. The two mice in which optogenetically-elicited USVs were observed are plotted as red circles. (C) Quantification of the proportion of CANE-ChR2-tagged PAG neurons that expressed Fos after 20 minutes of optogenetic stimulation (mean is 90 ± 2%, N = 10 mice).

Figure S6, related to Figure 6.

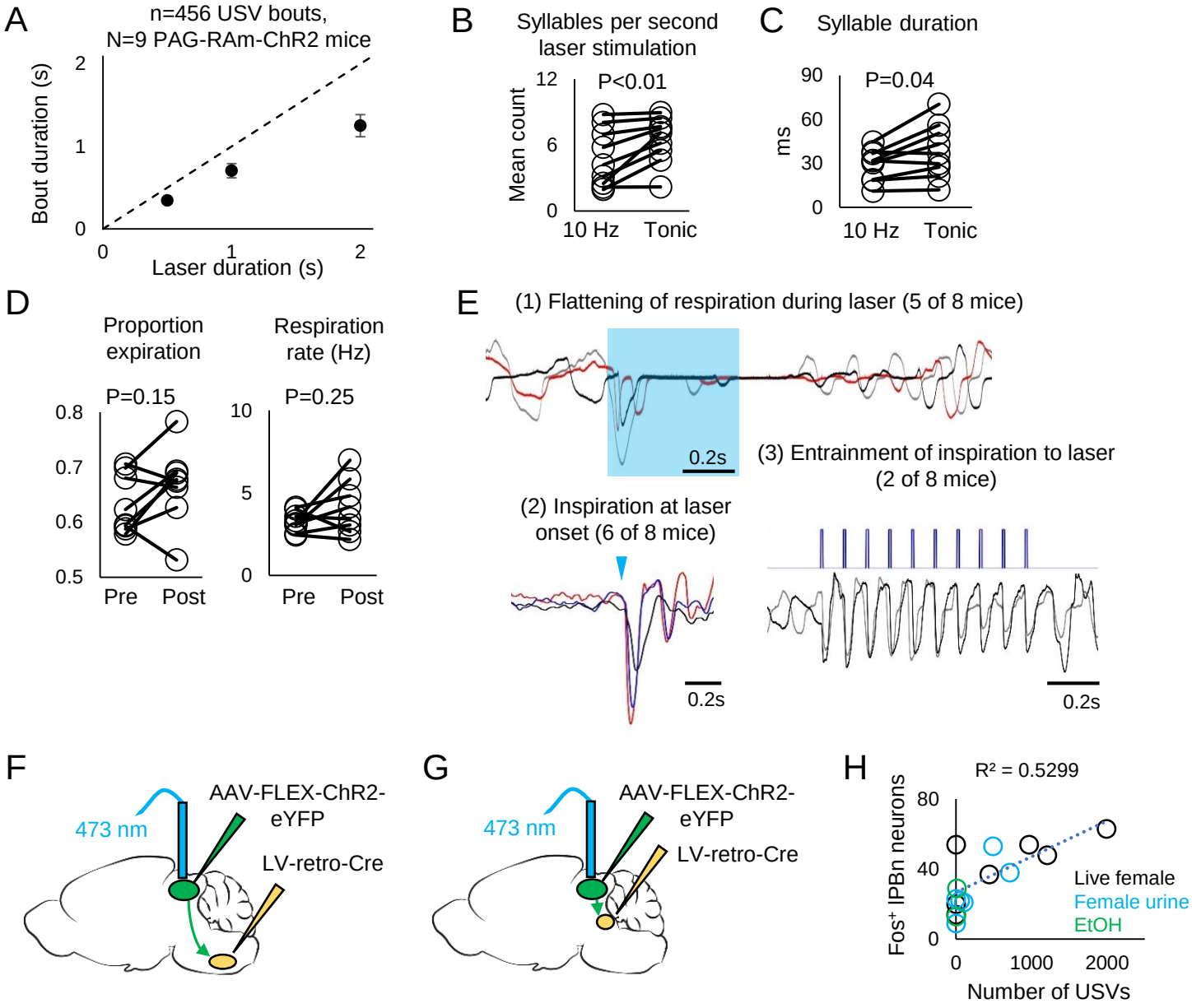

Figure S6, related to Figure 6. Additional information related to optogenetic activation of PAG-RAm and PAB-PBn neurons. (A) The duration of optogenetically-elicited bouts of USVs is similar to the duration of laser stimuli used to activate PAG-RAm neurons (n = 456 optogenetically-elicited USV bouts from N = 9 PAG-RAm mice. (B) Comparison of the number of USV syllables elicited per second of laser stimulation is shown for 10 Hz versus tonic laser stimuli for PAG-RAm mice ($p < 0.01$ for difference between 10 Hz and tonic, Wilcoxon signed-rank test). (C) Same as (B), except comparing mean syllable duration for USVs optogenetically elicited by 10 Hz and tonic laser stimuli ($p = 0.04$). (D) Optogenetic activation of PAG-RAm neurons caused no significant change in the proportion of the respiratory cycle occupied by expiration (left, n = 541 epochs of laser stimulation from N = 8 PAG_{RAm}-ChR2 mice, $p = 0.82$, Wilcoxon signed-rank test) and no significant change in respiration rate (right, $p = 0.25$). Breathing measurements made in 8 of 9 PAG_{RAm}-ChR2 mice. (E) Optogenetic activation of PAG-RAm neurons elicited heterogeneous effects on respiration, including: (top) a “flattening” of respiration (three example breathing traces shown for a representative PAG_{RAm}-ChR2 mouse); (bottom left) pronounced inspiration at laser onset (mean breathing aligned to onsets of all laser stimuli shown for N = 3 representative PAG_{RAm}-ChR2 mice); and (bottom right) entrainment of inspiration to phasic laser stimuli (two example breathing traces aligned to 5 Hz, 2s-long laser stimulus shown from a representative PAG_{RAm}-ChR2 mouse). We note that both PAG-RAm-ChR2 mice that exhibited entrainment of inspiration to laser stimuli had viral infection that extended caudally into the parabrachial nucleus, while the remaining N=7 mice that did not exhibit entrainment had viral labeling that was restricted to the PAG and surrounding reticular formation (data not shown). (F) Schematic showing the viral strategy used to express ChR2 in PAG-RAm neurons. (G) Schematic showing the viral strategy used to express ChR2 in PAG-PBn neurons. (H) Quantification of the number of USVs produced and number of Fos-positive PBn neurons in male mice that were exposed to various stimuli (live female social partner, black symbols; female urine; blue symbols, EtOH, green symbols).